ROYAL SOCIETY OF CHEMISTRY

Nanoscale

ARTICLE

Graphdiyne-supported single-cluster electrocatalysts for highly efficient carbon dioxide reduction reaction

Received 00th January 20xx,
Accepted 00th January 20xx

DOI: 10.1039/x0xx00000x

Pingji Ge,[a,b] Xingwu Zhai,[a,b] Xiaoyue Liu,[a,b] Yinglun Liu,[a,b] Xiaodong Yang,[a,b] Hongxia Yan,[a,b] Guixian Ge,[*,a,b] Jueming Yang,[*,a,b] and Yunhu Liu,[*,a,b]

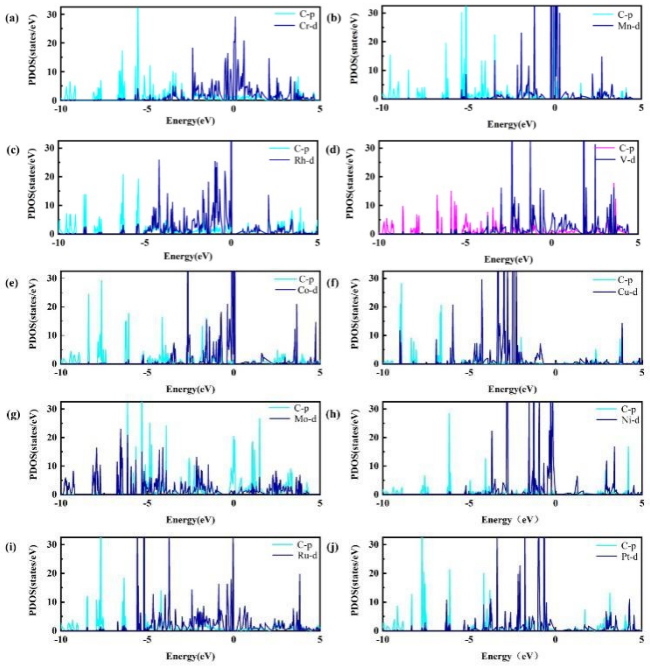

Fig.S1. Projected density of states (PDOS) of C-p orbital and TM-d orbital for TM_3@GDY.

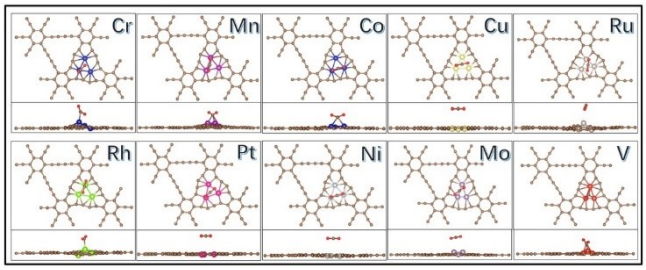

Fig. S2 The most stable configurations of top views and side views of adsorbed CO_2 on TM_3@GDY

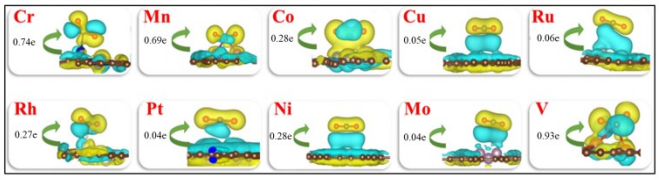

Fig. S3 The Bader charge analysis. The isosurface value is set to be 0.01 e/Å and the positive and negative charges are shown in yellow and cyan, respectively.

[a] *Key Laboratory of Ecophysics and Department of Physics, College of Science, Shihezi University North fourth Road, Shihezi City, P.R. China*
E-mail: geguixian@126.com,juemingyang11@gmail.com,liuyh@shzu.edu.cn
[b] *Xinjiang Production and Construction Corps Key Laboratory of Oasis Town and Mountain-basin System Ecology, Shihezi University North fourth Road, Shihezi City, P.R. China*
E-mail: geguixian@126.com,juemingyang11@gmail.com,liuyh@shzu.edu.cn
†Electronic Supplementary Information (ESI) available. See DOI: 10.1039/x0xx00000x

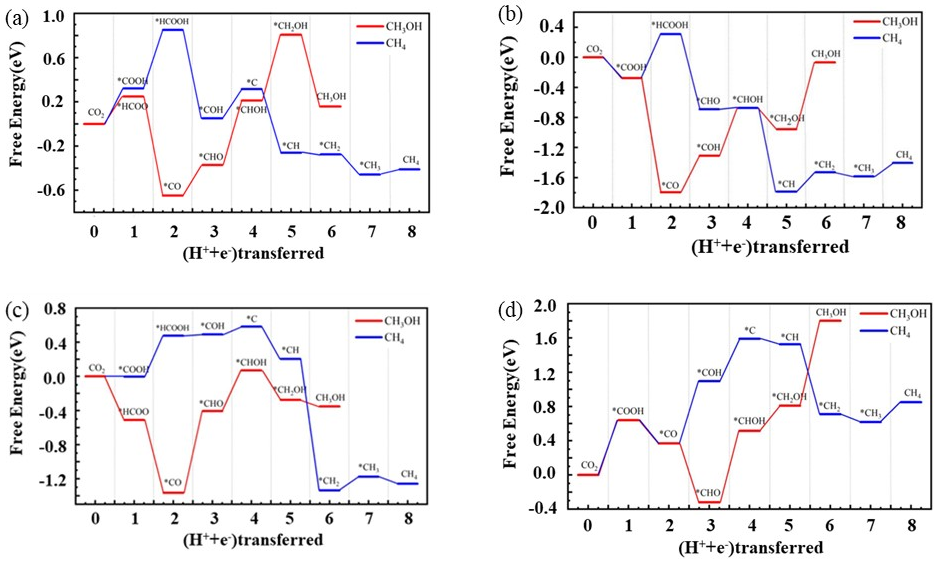

Fig. S4 Free-energy profiles for CO_2RR on **(a)**Mn_3@GDY, **(b)**Co_3@GDY, **(c)**Ru_3@GDY and **(d)**V_3@GDY.

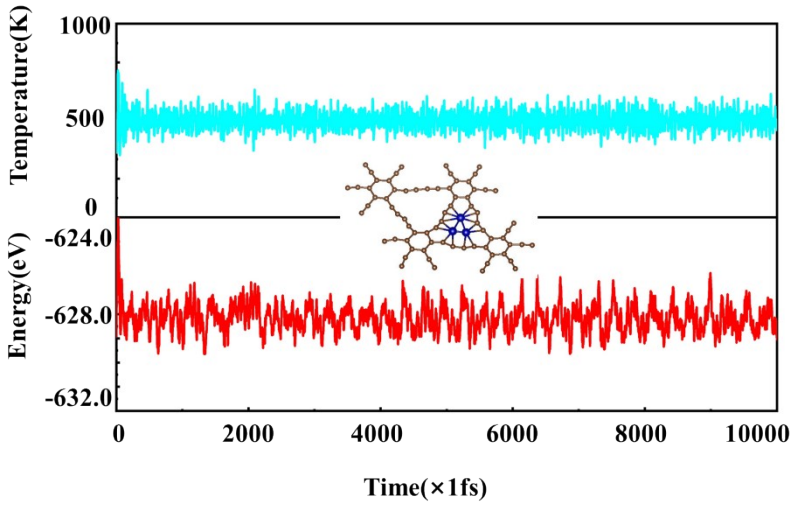

Fig. S5 The temperature and energy fluctuations of Cr_3@GDY during 10 ps of AIMD simulation. The insets illustrate the top and side view of Cr_3@GDY after 10 ps AIMD simulation at T = 500 K.

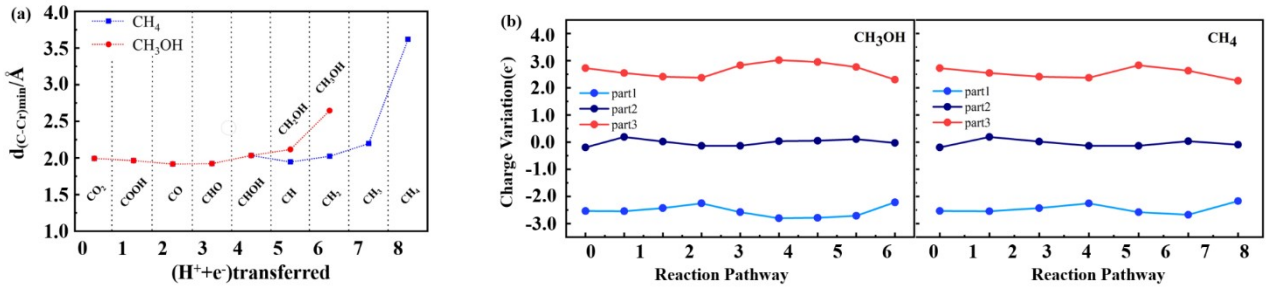

Fig. S6. (a) The variations of the C-TM (the closest TM atom of the adsorbed product) bond lengths through reaction pathway. **(b)**. The Bader charge analysis for three parts of Cr_3@GDY along the reaction pathway.

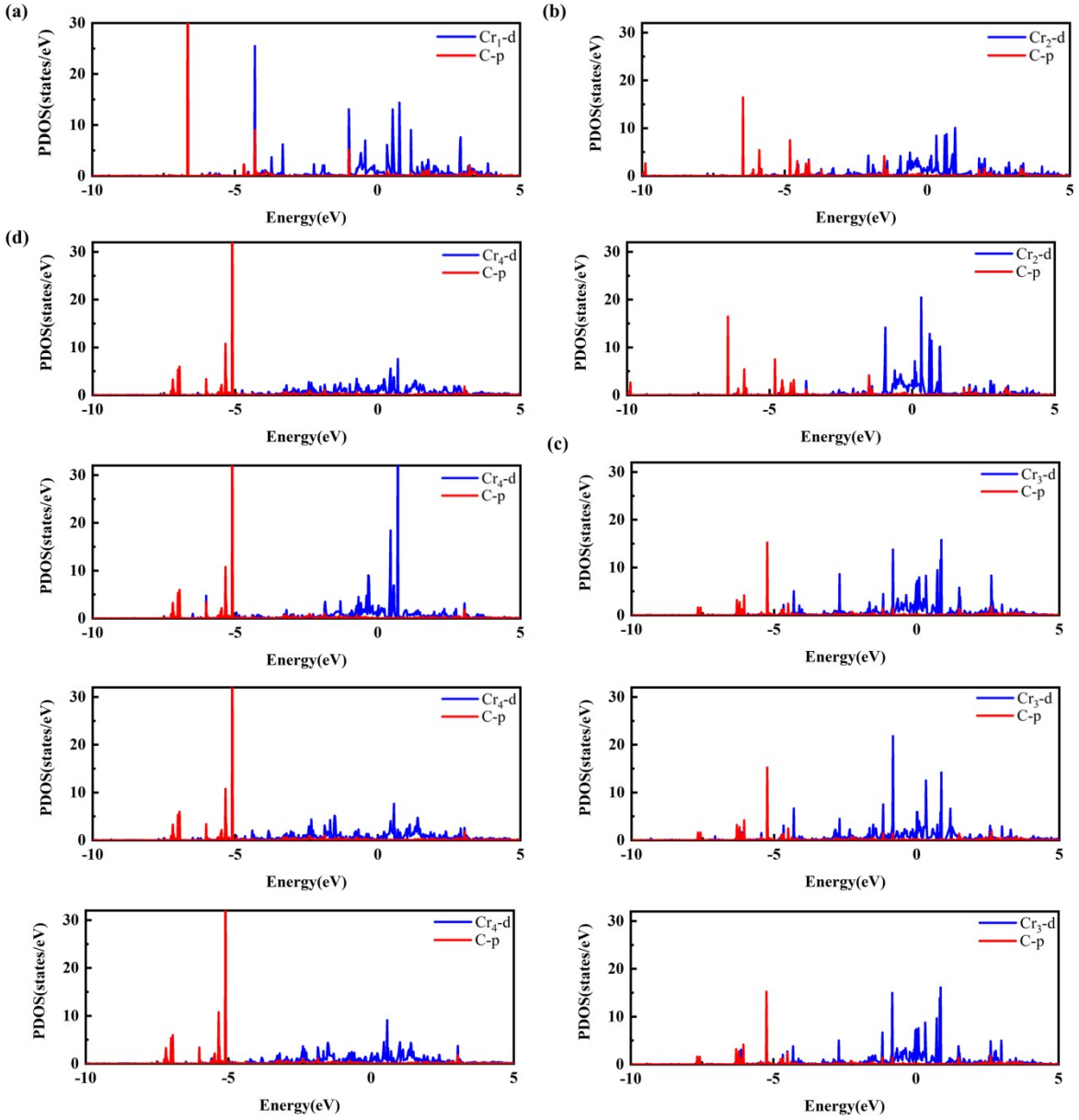

Fig.S7. Projected density of states (PDOS) of C-p orbital and Cr-d orbital of each Cr atom after CHOH generation on (a)Cr@GDY, (b)Cr_2@GDY, (c)Cr_3@GDY and (d)Cr_4@GDY.

Nanoscale

ARTICLE

Table S1. The binding energies (eV) of TM_3@GDY and cohesive energies (eV) of the corresponding bulk metal.

Catalysts	binding energies	cohesive energies
Mn_3@GDY	-9.34	-7.80
Cr_3@GDY	-8.48	-7.70
Co_3@GDY	-14.40	-9.44
Rh_3@GDY	-14.42	-25.84
Ru_3@GDY	-17.88	-14.78
V_3@GDY	-19.03	-14.54
Pt_3@GDY	-22.89	-22.19
Mo_3@GDY	-16.84	-14.72
Cu_3@GDY	-18.19	-14.84
Ni_3@GDY	-14.48	-21.84

Table S2. The adsorption energies (Eads, eV), O-C-O bond angles (angles, °), and charge transfers of CO_2 (Q, |e|) of the most stable CO_2 adsorption configurations on TM_3@GDY.

Catalysts	E_{ads}	angles	Q
Mn_3@GDY	-1.05	138.22	0.69
Cr_3@GDY	-0.79	137.12	0.74
Co_3@GDY	0.11	139.10	0.28
Rh_3@GDY	-0.21	179.57	0.04
Ru_3@GDY	-0.16	178.61	0.06
V_3@GDY	-1.24	155.07	0.27
Pt_3@GDY	-0.31	178.93	0.04
Mo_3@GDY	-0.22	179.40	0.04
Cu_3@GDY	-0.28	179.39	0.05
Ni_3@GDY	-0.24	128.57	0.83

Table S3. The maximum free energy change (ΔG_{max}, eV) and corresponding step of TM_3@GDY.

Catalysts	ΔG_{max}	Step
Mn_3@GDY	0.53	*CHO-*CHOH
Cr_3@GDY	0.39	*CHO-*CHOH
Co_3@GDY	0.48	*CO-*CHO
Rh_3@GDY	0.99	*CO-*CHO
Ru_3@GDY	0.48	*CHO-*CHOH
V_3@GDY	0.72	*CHO-*CHOH
Pt_3@GDY	2.09	*CO_2-*COOH
Mo_3@GDY	2.58	*CHO-*CHOH
Cu_3@GDY	1.26	*CO_2-*COOH
Ni_3@GDY	1.10	*CO_2-*COOH

Nanoscale

ARTICLE

Table S4. Energy change (ΔG, eV) of CO desorption and further reaction step for Cr_3@GDY.

step	ΔG
*CO-*CHO	0.30
*CO-*COH	1.91
CO desorption	1.45